

Influence of Co^{2+} Ions on Structural and Magnetic Properties of Co-Precipitated Mg-Cr Nanoferrite

S.Sukandhiya¹, B.Uthayakumar², S.Periandy³, R.Sujatha⁴, S.Uthiradevi⁵

^{1, 2, 4, 5} Research Scholar, Department of Physics, Kanchi Mamunivar center for PG Studies, Puducherry, India.

³ Associate Professor, Department of Physics, Kanchi Mamunivar center for PG Studies, Puducherry, India.

Abstract – Co^{2+} ions doped Magnesium - Chromium nanoferrite ($x= 0.0, 0.2, 0.4$ and 0.6) synthesized by Co-Precipitation method with pH as 10. Prepared samples are sintered at 1173K. Influence of Cobalt ion on structural and magnetic properties of $\text{Co}_x\text{Mg}_{1-x}\text{Fe}_{1.5}\text{Cr}_{0.5}\text{O}_4$ nano ferrite was reported here. The structural parameters were estimated by X- ray Diffraction (XRD). Morphology and composition of the synthesized samples has been evaluated Scanning Electron Microscope (SEM) and Energy Dispersive X-ray Spectroscopy (EDX) respectively. The spinel formation have been investigated by Fourier Transform Infrared Spectroscopy (FTIR) and two prominent absorption bands ν_1 and ν_2 corresponding to the stretching vibration of tetrahedral and octahedral sites around 600 cm^{-1} and 400 cm^{-1} . The magnetic parameter such as Saturation magnetization (M_s), Remanent magnetization (M_r), Coercive field (H_c) and Squareness ratio are determined by Vibrational Sample Magnetometer (VSM). The XRD pattern shows synthesized nano powder samples are having cubic spinel structure with average crystallite size ranging from 49 to 57 nanometers. It is found that the lattice constant, lattice strain, and dislocation density value non-linearly varies with increase in Co ions of Mg-Cr ferrite. The magnetic parameters changes with respect to increase in concentration of Co^{2+} ions. Maximum Anisotropy obtained at $x= 0.4$. Minimum coercivity value obtained at $x=0$ and $x=0.2$.

Index Terms – Co-Mg-Cr Ferrite, Co-Precipitation method, XRD, SEM, EDAX, FTIR, VSM.

1. INTRODUCTION

Ferrite materials have attracted the researchers for last few decades due to their extensive applications, ranging from fundamental research to industrial use [1,2]. MgFe_2O_4 is soft magnetic material n - type material [3]. Mainly soft magnetic property of ferrites materials acts as heterogeneous catalysis, adsorption, sensors, magnetic technologies[4], human cancer therapy[5]. Spinel ferrites have general molecular formula $(\text{A})[\text{B}_2]\text{O}_4$. Each spinel unit cell contains eight formula units. The larger oxygen anions form a close-packed face centered cubic structure with the smaller metal cations occupying the interstitial positions. There are two types of interstitial sites: the tetrahedral (8a) or (A) sites, and the octahedral (16d) or [B] sites, which are occupied by the metal cations [6,7]. This type of spinel structure show interesting structural and magnetic properties, which vary the ions, charge and site distribution among the tetrahedral, octahedral or both the sites [8].

The structural and magnetic properties of ferrites are found to be sensitive to their composition and microstructure, which in turn are dependent on the processing conditions and different synthesis routes [9]. Several chemical processing techniques are available for the synthesis of ferrites [10-14]. The selection of an appropriate synthetic procedure often depends on the desired properties and the final applications. Among these methods, Chemical co-precipitation was selected as a best method to synthesize nanoparticles. It is least expensive simplest approach for making nanoparticles, it produce large quantities (order of grams) in relatively short interval of time [15].

N.Thomas et al studied magnetic and electric properties of Magnesium substituted Cobalt ferrite ($x= 0$ to 1 in steps of 0.2) prepared by solution combustion method, when substituting Mg the transition from hard to soft magnetic nature is obtain, the coercivity value at $x =0.8$ and 1 is 325 and 89 Oe respectively [16]. In my previous study, Cobalt doped Nickel Chromium nanoferrite does not have superstructure peaks. At higher concentration of Co ions increase the magneto crystalline anisotropy constant value, which will release more thermal energy in alternating magnetic field. [17]. Doping Cobalt ions in Magnesium Chromium nanoferrite synthesized by Co-precipitation is the novel and it not reported yet. Present work is to investigate the physio-chemical behavior of Co^{2+} ions in MgCr nanoferrite with different concentrations.

2. MATERIALS AND METHODS

2.1 Material for synthesis

$\text{Co}_x\text{Mg}_{1-x}\text{Fe}_{1.5}\text{Cr}_{0.5}\text{O}_4$ nano ferrites at various concentration of Cobalt ion has been synthesized from Precursors CoCl_2 , $\text{MgCl}_2 \cdot 6\text{H}_2\text{O}$, $\text{CrCl}_3 \cdot 6\text{H}_2\text{O}$, $\text{FeCl}_3 \cdot 6\text{H}_2\text{O}$ and NaOH. Analytical grade of these precursors are purchased from SIGMA ALDRICH, Germany with 98% purity.

2.2 Synthesis Methodology

A successful synthesizing methodology involves correct choice of precursor, its composition and reaction environment. Particularly for wet chemical methods like sol-gel, hydrothermal, co-precipitation and colloid emulsion technique, pH controller plays an important role. For the present work eco friendly NaOH is used to maintain pH. The physio-chemical

properties of nanoparticles are greatly influenced by particle size, morphology, purity and chemical composition. Using chemical method, have been conformed to efficiently control the morphology and chemical composition of prepared nano powder. Among wet chemical techniques sol-gel, hydro thermal and colloid emulsions are time consuming and involve highly unstable alkoxides and difficult to maintain reaction conditions. Co-precipitation is one of the more successful techniques for synthesizing ultrafine nanoparticles having narrow particle size distribution [18]. These advantages on co-precipitation method motivated authors to synthesize $\text{Co}_x\text{Mg}_{1-x}\text{Cr}_{0.5}\text{Fe}_{1.5}\text{O}_4$ ($x = 0, 0.2, 0.4$ and 0.6) nano ferrites by co-precipitation method. The precursors for Fe ion are taken as 2 M and 1M for other Metals chlorides. They are mixed in stoichiometric ratio and added one by one on the basis of their electronegativity value. Mixture of Aqueous solution is stirred rigorously at 338K for 30 minutes, meanwhile NaOH is added to the brain solution by drop by drop using a burette till solution reaches pH value 10. The required composition of nano ferrites are formed from conversion of metal salt into hydroxide and then transformed into ferrites. The precipitates obtained were thoroughly washed more than three times with double distilled water and acetone. The final product were dried and sintered at 1173 K for the formation of spinel ferrite crystal structure.

2.3 Physical measurements

Crystal structure of all the samples were examined by powder X-Ray diffraction XRD patterns at room temperature PANalytical-X'Pert PRO powder diffractometer using $\text{Cu-K}\alpha_1$ radiation. Scanning Electron Microscopy (SEM) study was performed by VEGA 3 TESCAN Scanning Electron Microscope, operated at 120 KV. Elemental analysis has been done with BRUKER EDS. Fourier Transform Infrared (FT-IR) spectra were recorded on SHIMADZ FT-IR spectrophotometer using KBr pellets in the range $4000-400\text{ cm}^{-1}$. The magnetic properties were measured at room temperature by LAKESHORE vibrating sample magnetometer (VSM).

3. RESULT AND DISCUSSION

3.1 X - Ray Diffraction analysis

Fig.1 shows x-ray diffraction pattern of synthesized samples of Cobalt doped Magnesium-Chromium nano ferrite for the concentration $x = 0, 0.2, 0.4$ and 0.6 . Major peaks (220), (311), (400), (511) and (440) are present in XRD pattern which confirms the formation of cubic spinel ferrite. In addition to major peaks, minor reflections peaks (111), (422), and (620) are present in all samples. This match with the JCPDS file MgFe_2O_4 is 88-1943 [19], CoCr_2O_4 No. 780711 [20] and MgCr_2O_4 No is 10-351 [21]. The planes (111) is absent at $x=0.4$, (422) is absent in $x=0.6$, (620) absent in $x=0.2, 0.6$. This disappearance of minor reflection peaks are due to conversion of Fe^{2+} into Fe^{3+} induced by more number of Co^{2+} ions.[22,23] For these combination of samples no extra peaks are obtained

it indicates single cubic phase nature of the nanoferrite. At $x=0.2$, the superstructure peak (210) present with low intensity. Generally intensity of XRD peaks corresponds to the crystalline nature of the samples. At $x=0.6$ the intensity of XRD peaks higher than all other samples. Addition of higher ionic radius Co^{2+} ion ($r_{\text{Co}} = 0.74 \text{ \AA}$) in Mg-Cr nano ferrite which will influences the crystalline nature of all samples. Intensity and peak width of XRD pattern related to particle size and crystallinity of the samples. The intensities of (220) and (440) planes are more sensitive to cations in tetrahedral and octahedral sites respectively [22,23]. From TABLE 1 it is clear that intensity of (220) and (440) initially increases addition of Co^{2+} after that non-linearity occur on both sites, this is due to decrease in Magnesium ions at both site. And Fe^{2+} ion in the octahedral site formed due to reduction of Fe^{3+} ion to Fe^{2+} ions for higher Cobalt concentration.

Average crystallite size 'D' and lattice constant has been estimated from X-ray reflections indexed (111), (220), (311), (222), (400), (422), (511), (440) and (620), using Scherer's equation $D = 0.9 \lambda / \beta \cos \theta$, where D is the average crystallite size, β is the full width half maxima, λ is the X-Ray wavelength and θ is the Bragg's angle. Lattice constant has been calculated from equation $a = d (h^2 + k^2 + l^2)^{1/2}$ Where 'a' is lattice constant, d be the inter planar distance, hkl is miller indices. Lattice strain of $\text{Co}_x\text{Mg}_{1-x}\text{Cr}_{0.5}\text{Fe}_{1.5}\text{O}_4$ were determined using the Williamson-Hall formula $\epsilon = \beta / 4 \tan \theta$, Where ϵ is the lattice strain of the structure. X-ray Density can be calculated by $\rho_x = ZM/\text{Na}^3$, Where Z is number of molecules per unit cell, here it is 8. M is Molecular weight of the sample N is Avagadro's Number, 'a' lattice constant. Dislocation density has been found by using the relation $\delta = 15 \epsilon / a D$, here δ be the dislocation density [24]. All these structural parameters are calculated and tabulated in TABLE 2.

The average crystallite size 'D' estimated for $\text{Co}_x\text{Mg}_{1-x}\text{Cr}_{0.5}\text{Fe}_{1.5}\text{O}_4$ nanoferrites for different 'x' values lie in between 49 nm and 57 nm. The samples having lattice constant between 8.3078 \AA and 8.3436 \AA and this increases in lattice constant with increase in concentration of Cobalt is due to addition of higher ionic radius Co^{2+} ion ($r_{\text{Co}} = 0.74 \text{ \AA}$) which replaces the smaller ionic radius Mg^{2+} ion ($r_{\text{Mg}} = 0.72 \text{ \AA}$). Non-linearity in the values occur and it violates Vegard's law. Increase in Co^{2+} concentration leads to increase in average crystallite size. Variation in the crystallite size is generally due to the influence of dopant, here crystallite size and lattice constant increase initially after that vary is due to Co^{2+} ions prefers octahedral sites whereas Fe^{3+} and Mg^{2+} ions prefers both tetrahedral and octahedral sites. When the particle size reduced to nano dimension there is change in cation distribution Co^{2+} occupies both tetrahedral and octahedral sites. For concentration $x=0.6$ crystallite size is maximum with value of 57 nm. These phenomenons arise due to more strained and most dislocated sub-lattice created by Cobalt. Molecular weight of the $\text{Co}_x\text{Mg}_{1-x}$

$x\text{Cr}_{0.5}\text{Fe}_{1.5}\text{O}_4$ composition increases with replacement of higher atomic mass (58.93 gm) Co^{2+} by lower atomic mass (24.31 gm) Mg^{2+} in the composition and this matches with the X-Ray density values calculated from XRD profile.

3.2 Scanning Electron Microscope (SEM) and Energy Dispersive Spectroscopic (EDS) analysis

The morphological characteristics of the obtained $\text{Co}_x\text{Mg}_{1-x}\text{Cr}_{0.5}\text{Fe}_{1.5}\text{O}_4$ nanoferrites sintered at 1173 K have been investigated with the help of VEGA 3 TESCAN for all concentration of the samples. Fig.2 shows morphology of $\text{Co}_x\text{Mg}_{1-x}\text{Cr}_{0.5}\text{Fe}_{1.5}\text{O}_4$ nano ferrite samples for the increase in concentration of Cobalt ($x = 0, 0.2, 0.4, 0.6$). The micrographs show the morphology is almost uniform and regular shaped particles in all the concentration. The result of SEM is well in agreement with X-Ray diffraction pattern, $x = 0, 0.2, 0.6$ morphology shows fine particle nature. The surface of the ferrite samples has a number of fine pores or voids that are attributed to the large amount of Oxygen and chlorine gas liberated during the sintering process. Presence of vacancies results in contraction of Lattice even higher ionic radius dopant is added to the sample [25].

EDS spectrum for the $\text{Co}_x\text{Mg}_{1-x}\text{Cr}_{0.5}\text{Fe}_{1.5}\text{O}_4$ ($x = 0, 0.2, 0.4, 0.6$) nanoferrites are recorded with BRUKER EDS and illustrated in Fig.3. The result shows each peak corresponds to the element added in the prepared nanoferrite which confirmed the presence of elements in respective concentration. Iron and oxygen are the major constituents in the composition and Magnesium, Chromium and cobalt are the next major constituent to the iron in the sample. It is interesting to note that the preparation condition completely favours the formation of mixed ferrite and allow us to study the effect of increasing the Co content on the properties of the Mg-Cr nano ferrite. The peak values variation is due to its stoichiometry for all the concentration. The values of Magnesium vary with the increase in Cobalt concentration.

3.3. Fourier Transform Infrared Spectroscopy (FTIR) Analysis

Fourier transform infrared (FTIR) studies were carried out to ascertain the metal-oxygen bonding. FTIR spectrums of the investigated sample are shown in Fig.4. Infrared spectroscopy study supported the formation of Mg-Co-Cr spinel nano ferrite with enlightening two strong absorption bands around 400 cm^{-1} and 600 cm^{-1} that are common features of all spinel ferrites [26]. The spinel structure is attributed to the stretching vibrations of the unit cell of the spinel in the tetrahedral (A) Site and The metal-oxygen vibration in the octahedral (B) site. These absorption bands are highly sensitive to changes in interaction between oxygen and cations, as well as to the size of the obtained nano-particles [27]. The broadening of the spectral band depends on the statistical distribution of cations over A and B sites. The vibration frequency depends on the cation mass, cation-oxygen distance and bending force [28].

From Fig 4 and Table 3, Intrinsic stretching vibration frequency of metal-oxygen at tetrahedral site observed in a range 613 cm^{-1} - 610 cm^{-1} and its value shifting linearly toward higher frequency with increase in Co^{2+} concentration in the samples. And replacement of Mg^{2+} ions by bigger Co^{2+} in octahedral sites results in a slight increase in metal oxygen bond length and consequently increase the wave number of octahedral and tetrahedral sites by increasing substitution content [29, 30]. Octahedral peak observed in the range of 460 cm^{-1} - 452 cm^{-1} , decrease in the value is due to migration of ions towards tetrahedral site is occur. Intensity of the peaks corresponds to octahedral and tetrahedral bonds decrease for $x \leq 0.4$ and increase for 0.6. It is well known that the intensity ratio is function of change of dipole moment with the inter-nuclear distance. This value represents the contribution of ionic bond Fe-O in the lattice. So the observed increase and decrease in the absorption band intensity with increase in Cobalt content, is due to perturbation occurring in Fe-O bonds. The electronic distribution of Fe-O bonds greatly affected by the dopant Co^{2+} which is having comparatively bigger radius and high atomic weight (Co- 58.93 amu, Mg 24.31 amu).

3.4 Vibrational Sample Magnetometer (VSM) analysis

MH-loops reveals the magnetic properties of $\text{Co}_x\text{Mg}_{1-x}\text{Cr}_{0.5}\text{Fe}_{1.5}\text{O}_4$ nanoferrite ($x = 0, 0.2, 0.4, 0.6$). Hysteresis loops for the samples are recorded with LAKESHORE Vibrational sample magnetometer at 300 K with applied field as 30 KOe are shown in Fig.5. The value of anisotropy constant was calculated from Stoner-Wohlfarth relation as follows $H_c = K/M_s$ [31], Where H_c is the coercivity, M_s saturation magnetization and K magnetic anisotropy constant. Calculation of magnetic moment in bohr magneton was carried out using the following relation, $n_B = (\text{Molecular Weight} \times M_s) / 5585$ [32]. Magnetic parameters saturation magnetization (M_s), Remanence Magnetization (M_r), Coercivity (H_c), Squareness ratio, Magnetic anisotropy constant (K) and magneton number are calculated from Hysteresis loop and tabulated in TABLE 4.

Generally magnetic properties in the prepared sample arise from coupling between spin and orbital angular momentum (L-S coupling) and electron spin (S-S coupling) [33]. In the case of spinel nano magnetic ferrite material magnetic parameters are influenced by cation distribution, collinearity and non collinearity (canting) of spins on their surface, Crystallite size and dopant.

The hysteresis loop shows that all the samples show super paramagnetic nature having low coercivity value upto $x=0.4$. At $x=0.6$ it shows diamagnetic nature. The pure MgCrFeO and 0.2 concentration of CoMgCrFeO shows almost equal value, only slight increase in the initial after that all the magnetic parameter value gets increase. The obtained magnetization and hysteresis value is comparatively less than that of the reported value [16,34]. The presence of Co^{2+} influenced the higher

magnetization and higher coercivity value at $x = 0.4$. Remanence value increase with increase in Co^{2+} ion due to more number of incorporation of Co^{2+} ion on the sublattices. The magneto crystalline anisotropy constant value is higher for high for larger saturation magnetization value, which is important to hold magnetic ions in certain direction, has been overcome by thermal energy [35]. The magnetic anisotropy constant maximum for the concentration 0.4 with less crystallite size and no superstructure peaks are obtained. Thus VSM result matches with XRD result.

4. CONCLUSION

$\text{Co}_x\text{Mg}_{1-x}\text{Cr}_{0.5}\text{Fe}_{1.5}\text{O}_4$ ($x = 0, 0.2, 0.4, 0.6$) nanoferrites were successfully synthesized by easy and simple co-precipitation method with average crystallite size between 49 nm and 57 nm. All physical properties are studied for samples sintered at 1173K. Addition of Co^{2+} ion influenced the structural properties such as Average crystallite size, lattice constant, lattice strain, dislocation density and X-Ray density of the synthesized samples. Absence of super structure reflection peaks from XRD analysis suggests that nano crystal lattice having disordered spinel structure in the higher concentration of the dopant. SEM shows uniform spherical shape manipulated by Co^{2+} ion in the sample and FTIR observation have fine match with results of XRD and conforms the cubic spinel ferrite. From VSM analysis Co^{2+} ions increase the magnetic parameter values. Important finding in this work is 0 and 0.2 concentration of Cobalt in Mg-Cr in nano ferrite has its minimum coercivity value and $x = 0.4$ has larger magnetic anisotropy constant value, which will release more thermal energy in alternating magnetic field, and should be act as best candidate for magnetic fluid hyperthermia and in targeted drug delivery system.

REFERENCES

[1] Y. Liu, Y. Zhong, J. Zhang, Z. Ren, *J. Appl. Phys*, 110, (2011) 074310
 [2] P.K.Roy, J.Bera, *J. Magn. Magn. Mater.* 298, (2006) 38
 [3] R.J. Willey, P.Noirclerc, G. Busca, *Chem, Eng. Commun.* 123 (1993) 1-16
 [4] S.K. Pradhan, S.Bid, M.Gateshki, V.Petkov, *Materials Chemistry and Physics* 93 (2005) 224-230

[5] Y.Watanabe, K.Sato, S.Yukumi, M.Yoshida, Y.Yamamoto. *Bio-Med.Mater.Eng.*19 (2009) 101-110
 [6] V.Stevanovic, M. d'Avezac, A. Zunger, *Phys, Rev, Lett.* 105 (2010) 075501
 [7] H.T.Jeng, G.Y. Guo, D.J.Huang, *Phys, Rev. Lett.* 93 (2004) 156403
 [8] J.B.Goodenough, *Magnetism and the Chemical Bond*, John Wiley, New York. London, 1963, p, 120
 [9] P.P. Hankare, R.P. Patil, K.M. Garadkar, R.Sasikala, *Mater.Res.Bull.* 46 (2011) 447
 [10] J.Giri, T.Sriharsha, D.Bhadur, *J.Mater.Chem.*14 (2004) 875
 [11] M.George, A.M. John, S.S.NAir, P.A. Joy, *J.Magn.Magn.Mater.*302 (2006) 190
 [12] J.Wang, *Mater.Sci.Eng. B* 127, (2006) 81
 [13] P.P.Hankare, V.T.Vader, N.M.Patil, S.D.Jadhav, *Mater,Chem,Phys* 113 (1) (2009) 233.
 [14] S.Z.Zhang, G.L.Messing, *J.Am.Cerm. Soc.* 73 (1990) 61
 [15] H.Shokrollai, *Journal of Magn. Magn Mater* 320 (3-4) (2008) 463-474
 [16] N.Thomas, P.V.Jithin, V.D.Sudheesh, V.Sebastian *Ceramic International*
 DOI: 10.1016/j.ceramint.2017.03.031 (In Press)
 [17] S.Sukandhiya, B.Uthayakumar, S. Periandy *IOSR, J. of Applied Phys* 9, (issue 3, Ver IV) (2017) 4-12
 [18] T.F.Marinca, I.Chicinas, O.Isnard, V.Pop, F.Pop, *J.Alloys and compds*, 509 (2011) 7931-7936.
 [19] S.K.Durrani, S.Naz, M.Mehmood, M.Nadeem *J of Saudi Chemical Society* 21 (2017) 899-910
 [20] C. Rath, P.Mohanty, A.Banerjee *J.of Magn. Magn. Mater* 323 (2011) 1698-1702
 [21] X. Duan, J.Liu, X.Wang, H.Jiang. *Optical Materials* 37 (2014) 854-861
 [22] B.P. Ladgaonkar, A.S. Vaigainkar, *Materials Chemistry and Physics* 56 (1998) 280-283
 [23] C.S.Narasimhan, C.S.Swamy, *Physica Status solidi* 59 (1980) 817
 [24] B.Uthayakumar, S.Sukandhiya, J.Suryakumary, S.Periandy. *IOSR. J of Appl. Phys* 9 (5) (2017) 5-12
 [25] S.Prabhar, M.Dhanam, *J.Cryst.Growth* 41, 1-2 (2005) 285
 [26] M. Hashim, S.E.Shirsath, S. Kumar, R. Kumar *J. of alloys and compounds* 549 (2012) 348-357.
 [27] M.Farid, I.Ahmad, S.Aman, S.Kanwal, M.Murtaza, G.Alia *Journal of Ovanic research* 11 (2015) 1
 [28] A.M.Wahba, M.B.Mohammad, *Ceramic International* 40 (2014) 6127-6135.
 [29] A.G.Boshale, B.K.Chougule. *Materila Chemistry and Physics* 97 (2006) 273
 [30] J.Smit, H.P.Jijn, *Ferrite* (1959)
 [31] N.Singh, A.Agarwal, S.Sanghi, P.Singh, *Physica B* 406 (2011) 687
 [32] S.Singhal, K.Chandra, *J.Solid State Chem* 180 (2007) 296
 [33] M.A.Gabbal, Y.M.A.Angari, *MaterilChem Physics* 118 (2009) 153
 [34] K.Ramarao, B. Rajesh Babu, K.Babu, S.D.Ramarao *Physica B: Phys of Condensed Matter* (2017) DOI: 10.1016/j.physb.2017.10.072
 [35] A.Verma, T.C.Goel, R.G.Meadiratta, P.Kishan *J.Magn.Magn.Mater* 208 (2000) 13-19

TABLE 1: Comparison of X-Ray Intensity

Co content 'x'	Composition	I ₂₂₀	I ₄₄₀
0.0	Mg _{1.0} Cr _{0.5} Fe _{1.5} O ₄	28.05	52.10
0.2	Co _{0.2} Mg _{0.8} Cr _{0.5} Fe _{1.5} O ₄	34.55	61.64
0.4	Co _{0.4} Mg _{0.6} Cr _{0.5} Fe _{1.5} O ₄	29.68	59.09
0.6	Co _{0.6} Mg _{0.4} Cr _{0.5} Fe _{1.5} O ₄	34.35	52.74

TABLE 2: Structural parameters of $\text{Co}_x\text{Mg}_{1-x}\text{Cr}_{0.5}\text{Fe}_{1.5}\text{O}_4$ for various concentrations sintered at 1173K

Co content 'x'	Composition	Crystallite Size D (nm)	Lattice Constant a (Å)	Molecular Weight g/mole	X-ray density g/cm^3	Lattice strain 10^{-3}	Dislocation Density 10^{15}
0.0	$\text{Mg}_{1.0}\text{Cr}_{0.5}\text{Fe}_{1.5}\text{O}_4$	50.26	8.3158	198.02	4.5745	2.662	1.2622
0.2	$\text{Co}_{0.2}\text{Mg}_{0.8}\text{Cr}_{0.5}\text{Fe}_{1.5}\text{O}_4$	50.373	8.3436	204.94	4.6872	2.316	0.8701
0.4	$\text{Co}_{0.4}\text{Mg}_{0.6}\text{Cr}_{0.5}\text{Fe}_{1.5}\text{O}_4$	49.91	8.3078	211.86	4.9084	2.029	1.0123
0.6	$\text{Co}_{0.6}\text{Mg}_{0.4}\text{Cr}_{0.5}\text{Fe}_{1.5}\text{O}_4$	57.014	8.3366	218.78	5.0164	2.205	0.7108

TABLE 3: Vibrational frequency of tetrahedral and octahedral sites

Co content 'x'	Composition	ν_{tetra}	ν_{octa}
0.0	$\text{Mg}_{1.0}\text{Cr}_{0.5}\text{Fe}_{1.5}\text{O}_4$	612.28	460.37
0.2	$\text{Co}_{0.2}\text{Mg}_{0.8}\text{Cr}_{0.5}\text{Fe}_{1.5}\text{O}_4$	610.70	455.02
0.4	$\text{Co}_{0.4}\text{Mg}_{0.6}\text{Cr}_{0.5}\text{Fe}_{1.5}\text{O}_4$	612.89	452.69
0.6	$\text{Co}_{0.6}\text{Mg}_{0.4}\text{Cr}_{0.5}\text{Fe}_{1.5}\text{O}_4$	613.03	457.53

TABLE 4: Magnetic parameters of $\text{Co}_x\text{Mg}_{1-x}\text{Cr}_{0.5}\text{Fe}_{1.5}\text{O}_4$ for various concentrations sintered at 1173K

Co content 'x'	Composition	M_s (emu/g)	M_r (emu/g)	H_c (Oe)	M_r/M_s	K (erg/cm ³)	n_B
0.0	$\text{Mg}_{1.0}\text{Cr}_{0.5}\text{Fe}_{1.5}\text{O}_4$	6.40	3.72	48.0	0.581	307.2	0.2270
0.2	$\text{Co}_{0.2}\text{Mg}_{0.8}\text{Cr}_{0.5}\text{Fe}_{1.5}\text{O}_4$	6.41	3.82	48.0	0.595	307.68	0.2354
0.4	$\text{Co}_{0.4}\text{Mg}_{0.6}\text{Cr}_{0.5}\text{Fe}_{1.5}\text{O}_4$	21.65	13.08	240.2	0.604	5200.33	0.8214
0.6	$\text{Co}_{0.6}\text{Mg}_{0.4}\text{Cr}_{0.5}\text{Fe}_{1.5}\text{O}_4$	0	0	0	0	0	0

M_s - Saturation magnetization; M_r - Remanent Magnetization; H_c - Coercivity; K - Magneto Crystalline Anisotropy; n_B - Magneton Number

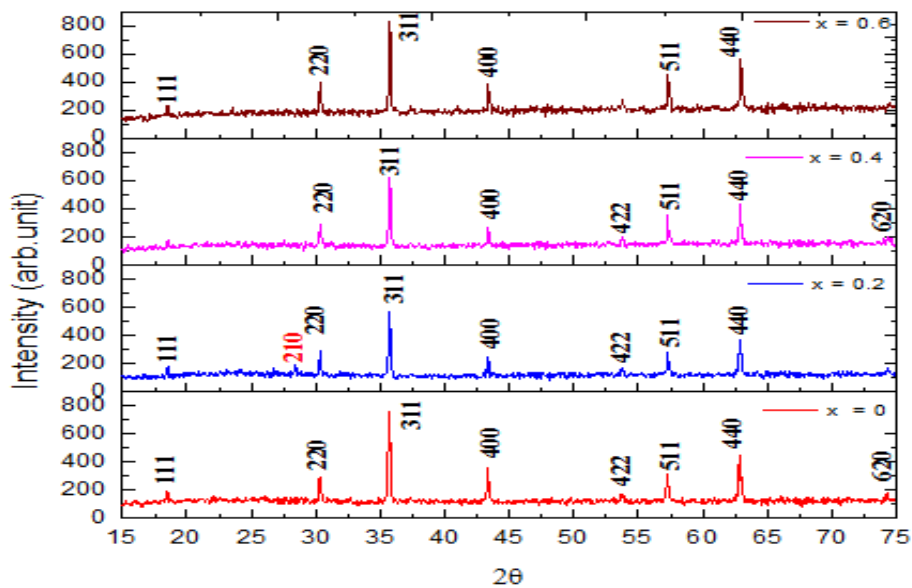


Figure 1: X-Ray Diffraction pattern of Co doped Mg-Cr nano ferrite samples

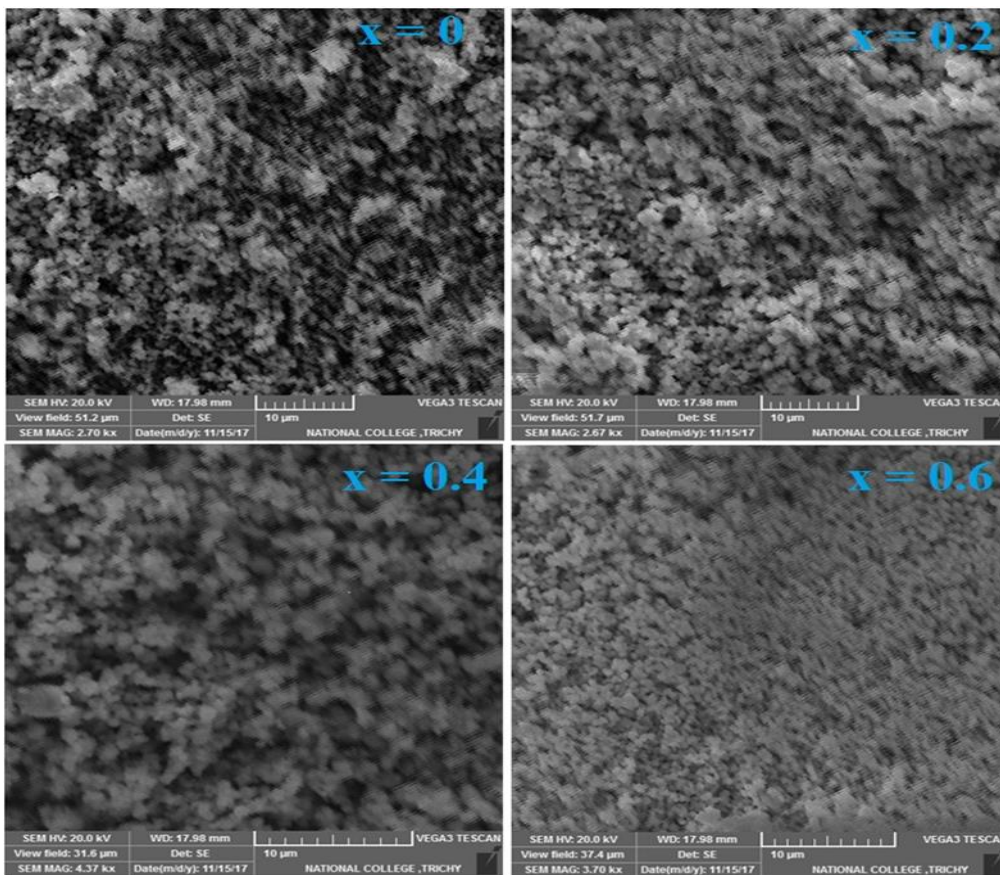


Figure 2. SEM micrograph of $Co_xMg_{1-x}Cr_{0.5}Fe_{1.5}O_4$ ($x = 0, 0.2, 0.4, 0.6$) nanoferrite sintered at 1173K

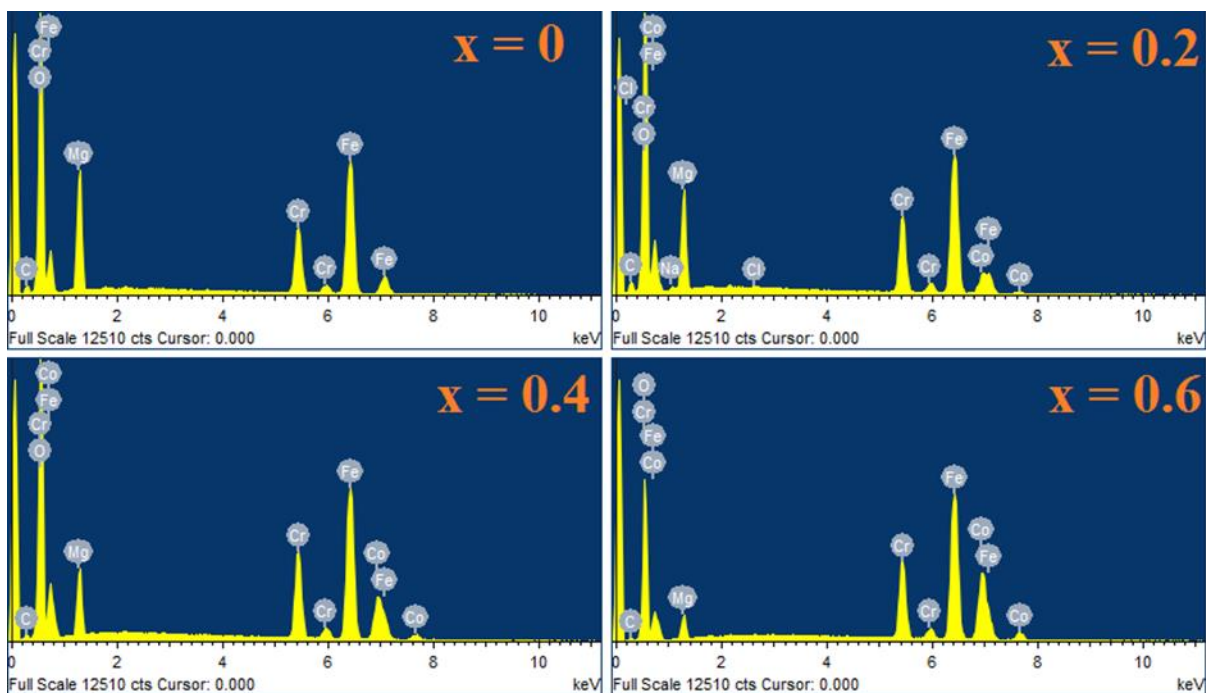


Figure 3. EDS of $\text{Co}_x\text{Mg}_{1-x}\text{Cr}_{0.5}\text{Fe}_{1.5}\text{O}_4$ ($x = 0, 0.2, 0.4, 0.6$) nanoferrite sintered at 1173K

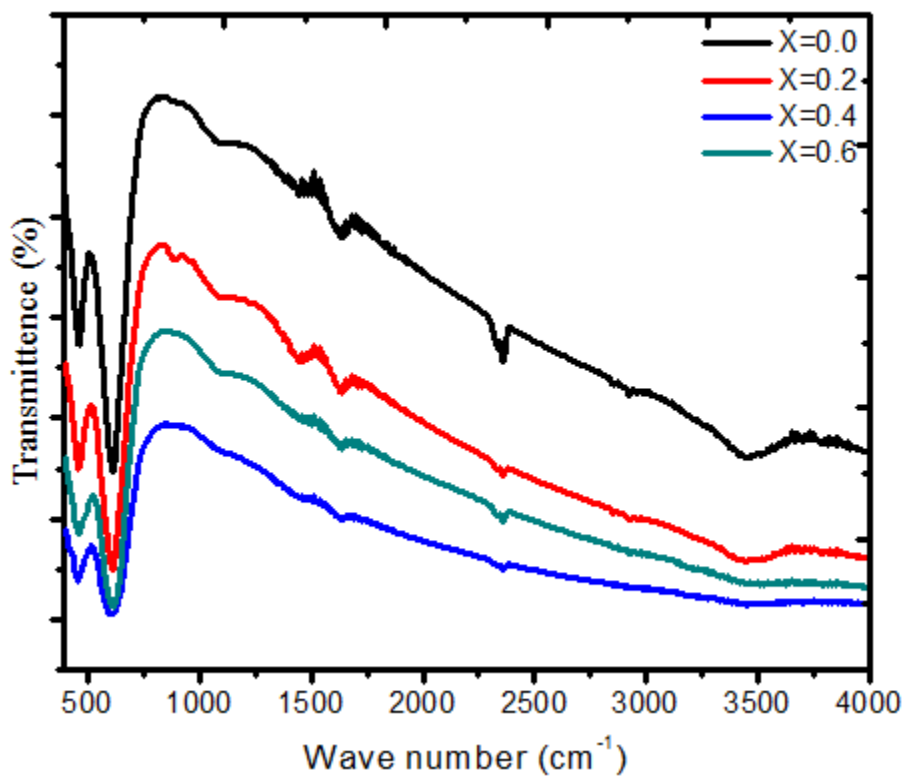


Figure 4. FTIR spectra of $\text{Co}_x\text{Mg}_{1-x}\text{Cr}_{0.5}\text{Fe}_{1.5}\text{O}_4$ ($x = 0, 0.2, 0.4, 0.6$) nanoferrite sintered at 1173K

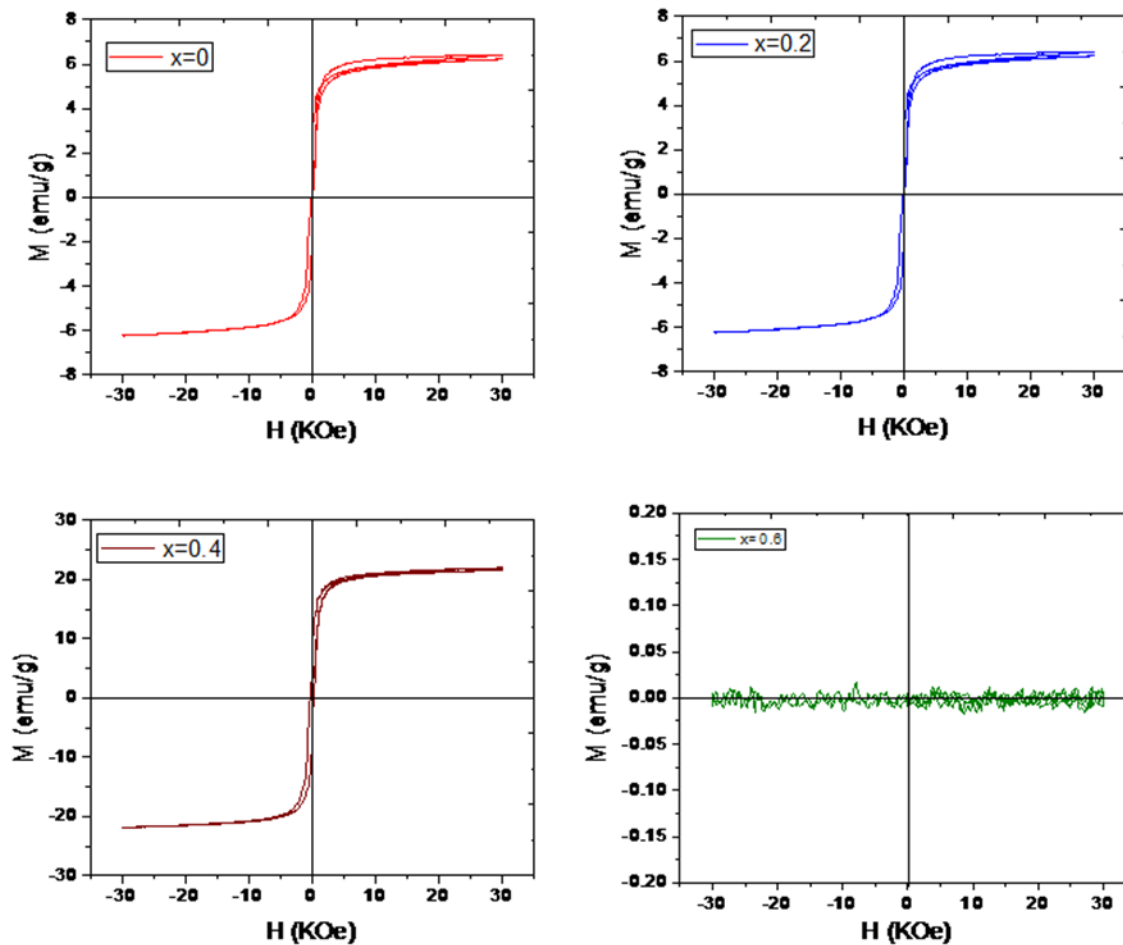


Figure 5. Magnetic hysteresis curves of $\text{Co}_x\text{Mg}_{1-x}\text{Cr}_{0.5}\text{Fe}_{1.5}\text{O}_4$ ($x=0, 0.2, 0.4, 0.6$) sintered at 1173K